Appendix S1: *Daphnia* foraging rate is not affected by presence or density of parasites.

In this appendix, we provide additional methods and results regarding the influence of parasite density on *Daphnia* foraging rate.

Methods: We conducted a preliminary experiment to examine how *Daphnia* foraging rates responded to the presence and density of fungal spores. In this experiment, we estimated the foraging rate of *Daphnia* consuming algae under four treatments ($N = 20$ per treatment; Control (algae only), algae + 100 fungal spores/mL, algae + 200 fungal spores/mL, and algae + 200 μg Cu^{2+} /L [Copper is a common pollutant that can potently alter *Daphnia* feeding rates (Bossuyt & Janssen 2004; Civitello *et al.* 2012). We used it here as a positive control]). Because *Daphnia* are nonselective feeders, they should forage on algae and spores at equal rates. We placed individual, 7-day-old *Daphnia* (same clonal genotype as in the infection experiment) in 10-mL filtered lake water containing 1.0 mg dry weight *S. acutus*/L in 15 mL borosilicate glass test tubes with plastic caps. We then allowed the *Daphnia* to consume algae for two hours under dark conditions in a closed cabinet in the laboratory (approximate temperature: 21°C). We mixed the tubes every 15 minutes by gently inverting them. After two hours, we quickly removed all *Daphnia* and estimated the density of algae remaining (A_2) using *in vivo* fluorometry (Trilogy Flourometer, Turner Designs, Sunnyvale, CA, USA). Algal density estimates obtained from *Daphnia*-free controls served as estimates of the initial density of algae (A_0). We calculated the foraging rate of each *Daphnia* (f, L ind^{-1} day^{-1}) following Sarnelle and Wilson (2008),

$$f = \frac{\ln(A_0 / A_2)V}{nt} \qquad \text{(Eq. S1)}$$

with container volume, $V = 0.010$ L, *Daphnia* per tube, $n = 1$, and time, $t = 0.0833$ day. We then tested for differences among these four treatments with ANOVA followed by post hoc Tukey tests to identify significantly different treatments. Three samples were lost before we could estimate the density of algae remaining. Therefore, we omitted these replicates from the analysis.

<u>*Results and Discussion*</u>: *Daphnia* foraging rate varied significantly among the four treatments (ANOVA, $F_{3,73} = 2.97$, $P = 0.037$). The addition of 100 or 200 fungal spores/mL did not alter foraging rate when compared to the "Algae only" treatment (Figure S1, $P = 0.50$ and $P = 0.98$, respectively). In contrast, copper significantly reduced the foraging rate of *Daphnia*. (Figure S1.1, $P = 0.041$). The confirmed effect of this positive control suggests that this assay can detect changes in *Daphnia* foraging rates. Therefore, we conclude that neither the presence nor density of fungal spores alters *Daphnia* foraging rates.

References

1. Bossuyt B.T.A. & Janssen C.R. (2004). Influence of multigeneration acclimation to copper on tolerance, energy reserves, and homeostasis of *Daphnia magna* straus. *Environ. Toxicol. Chem.,* 23, 2029-2037.
2. Civitello D.J., Forys P., Johnson A.P. & Hall S.R. (2012). Chronic contamination decreases disease spread: a *Daphnia*-fungus-copper case study. . *Proc. R. Soc. B,* 279, 3146-3153.
3. Sarnelle O. & Wilson A.E. (2008). Type III functional response in *Daphnia*. *Ecology,* 89, 1723-1732.

Appendix figure

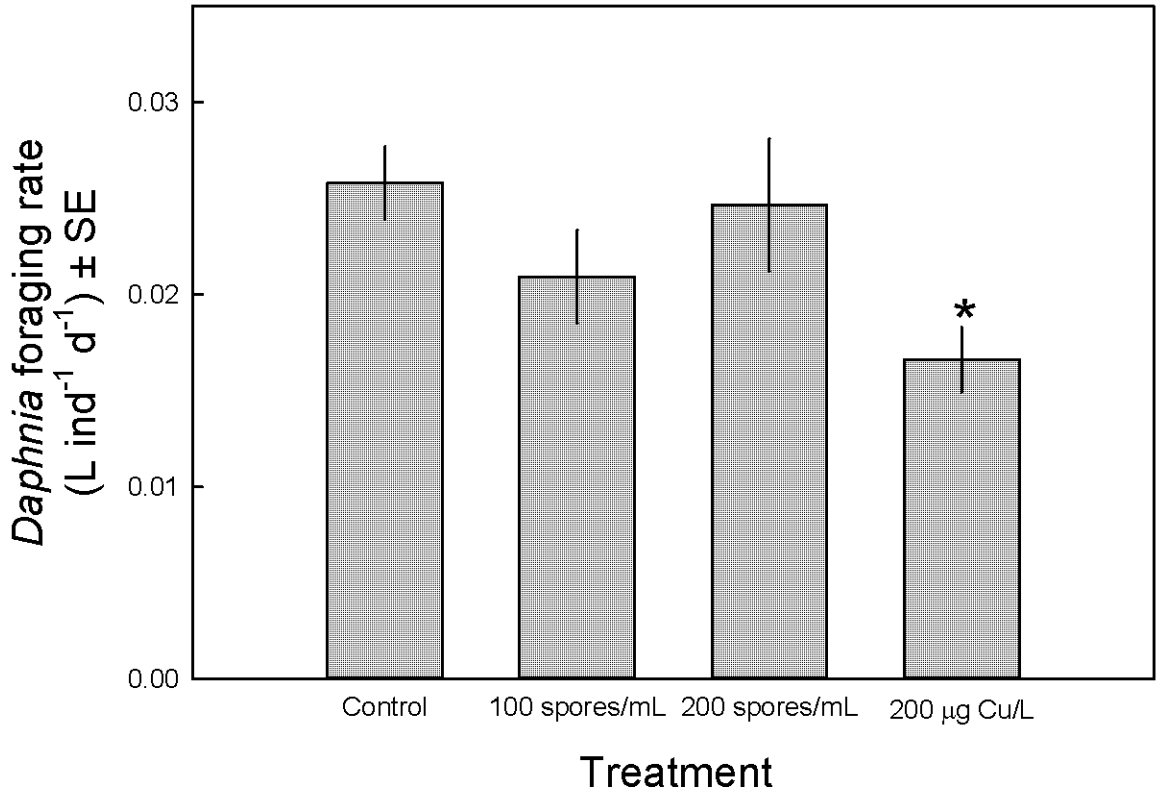

Figure S1.1. Results of the preliminary foraging rate assay. Parasite addition (i.e., the "100 spores/mL" and "200 spores/mL" treatments) had no significant effect on the foraging rate of *Daphnia* relative to the Control treatment. In contrast, the addition copper ("200 µg Cu/L treatment"), a common aquatic pollution that often reduces the foraging rates of aquatic invertebrates, significantly decreased *Daphnia* foraging rates. Foraging rates are presented as means ± SE. Significant differences from the "Algae only" control group are indicated by asterisks.

Appendix S2: Additional model selection methods and results for the infection experiment.

Here we describe methods for parameter estimation and model selection when combining infection and parasite consumption data (*Model Competition 2*). We provide maximum likelihood parameter estimates for all models in both analyses. We also provide confidence intervals for all parameter estimates from *Model Competition 2*. Finally, we provide best-fit predictions for some models that we not presented in the main text.

Additional methods for estimating parasite density in water samples

In order to more directly estimate *Daphnia* foraging rates in *Competition 2* (below), we measured the density of spores remaining in the water (i.e., those that were not consumed) after the one day exposure. We collected a 40 mL sample of well mixed water from 65 replicates at the two highest spore densities; stained the suspension with a cotton blue-lactic acid dye; filtered the samples onto 25-mm nitrocellulose filters (Millipore, Billerica, MA, USA); and counted the spores in at least 20 fields on each slide at 200x magnification on a compound microscope. We also estimated the initial density of spores using 12 additional replicates containing spores but no *Daphnia.*

Additional methods for model parameterization and competition

Here we provide more complete information concerning the parameterization and competition of the transmission models using data from the infection experiment. We fit and competed the transmission models twice. For both analyses, we used maximum likelihood

techniques to parameterize the models and standard information criteria for the competition (Burnham & Anderson 2002).

Competition 1: We first fit and competed all five models using only the infection data and assuming a betabinomial distribution ("Infection data only," Table 1B, Figure 1). In general, we followed standard maximum likelihood methods for fitting transmission models to data resulting from infection experiments (e.g., Hall *et al.* 2007; Rachowicz & Briggs 2007; Ben-Ami *et al.* 2008). For each model, we determined the parameter values that best predicted the prevalence of infection observed across all of the treatments. To predict prevalence, we integrated each model for the one day duration of the infection experiment. We found analytical solutions for all transmission models except for the *Phenomenological* model (Eq. 3a-b), which we numerically simulated with the lsoda function in the deSolve package within R Statistical Computing Software (R Development Core Team 2008; Soetaert *et al.* 2010). Integrating each transmission model provided a predicted density of susceptible hosts remaining after the one day exposure, $S(1)$, given the parameter values and initial densities of hosts, $S(0)$, and parasites, $Z(0)$. Dividing this prediction by the initial density of hosts, $S(0)$, provides the predicted probability of successfully escaping infection, p:

$$p = \frac{S(1)}{S(0)} = 1 - prevalence \qquad \text{(Eq. S2.1)}$$

The model predictions depended on model parameters as well as the initial densities of susceptible hosts, $S(0)$, and parasites, $Z(0)$:

Density dependent: $$p = \exp\left(-\beta Z(0)\right) \qquad \text{(Eq. S2.2a)}$$

Constant foraging: $$p = \exp\left(\frac{uZ(0)}{S(0)}\left(\exp\left(-fS(0)\right) - 1\right)\right) \qquad \text{(Eq. S2.2b)}$$

Linear interference: $$p = \exp\left(\frac{uZ(0)}{S(0)}\left(\exp\left(-f\left(1 - c_f S(0)\right)S(0)\right) - 1\right)\right) \quad \text{(Eq. S2.2c)}$$

Exponential interference: $$p = \exp\left(\frac{uZ(0)}{S(0)}\left(\exp\left(-f\left(\exp\left(-c_f S(0)\right)\right)S(0)\right) - 1\right)\right) \quad \text{(Eq. S2.2d)}$$

We assumed that the observed counts of uninfected *Daphnia*, U, followed a betabinomial distribution, with the probability of successfully escaping infection, p, predicted by the model. The betabinomial distribution also includes an overdispersion parameter, θ, which we estimated along with the model parameters. The betabinomial probability density function provides a likelihood for a parameter set based on the model-predicted success, p, and the number of uninfected hosts, U, observed among the total number of hosts, N, diagnosed in a replicate:

$$\ell_{INF}\left(\text{parameters} \mid \text{data}, \text{model}\right) = \binom{N}{U} \frac{\beta(N - U + \theta(1 - p), U + \theta p)}{\beta(\theta(1 - p), \theta p)} \quad \text{(Eq. S2.3)}$$

Here, $\beta(a, b)$ indicates the probability density function of the beta distribution with parameters a and b. To find the negative log-likelihood, $\mathcal{L}_{INF}$, for a specific set of model parameters given a model and the infection data, we summed the negative log-likelihood (i.e., $-\ln(\ell_{INF})$) calculated for the counts, U and N, from each replicate tube. We obtained maximum likelihood estimates of model parameters by minimizing this total using the betabinomial distribution from the emdbook package and the mle2 function of the bbmle package in R (Bolker 2008; R Development Core Team 2008; Bolker 2012).

After fitting each model, we ranked their performance with statistics derived from the Akaike information criterion (AIC; Burnham and Anderson 2002). The best performing model, by definition, has the lowest AIC value (AIC_{best}). Thus, we determined each model's performance (AIC_j) relative to the best, ($\Delta AIC_j = AIC_j - AIC_{best}$). By definition, $\Delta AIC_{best} = 0$, and larger ΔAIC_j correspond to worse model performance. Generally, $\Delta AIC > 10$ indicates poor

model performance (Burnham & Anderson 2002). We also calculated the Akaike weight, w_j, for each model from these AIC statistics. Akaike weights provide the relative weight of evidence in favor of a model among the set under consideration (Burnham & Anderson 2002). Akaike weights close to one indicate substantial evidence that the model performs best among the candidates, while w_j close to zero indicate extremely little support for the model.

Competition 2: Next, we used an integrated modeling approach to simultaneously fit the three foraging-based transmission models (*constant foraging, linear interference,* and *exponential interference*) to the infection and parasite consumption datasets. Each of these models simultaneously predicts infection prevalence (as above) as well as the density of parasite spores remaining (i.e., not consumed) after the one day exposure. In *Competition 2,* we estimated parameters by simultaneously fitting the models to these two datasets (Integrated modeling; Besbeas *et al.* 2005; Schaub *et al.* 2007). Combining multiple sources of data into a single model facilitates better parameter estimates, particularly when certain parameters may be difficult to estimate accurately with only a single source of data (i.e., when parameters have low identifiability). This advantage likely applies here because the parasite consumption data can more directly inform the foraging parameters (f and c_f) than can the infection counts. Here, we make the (relatively standard) assumption that the infection counts and parasite density estimates are independent. Thus, the joint likelihood (which we maximize in this simultaneously fit) is the product of the individual likelihoods for each dataset (or, alternatively, as the sum of the log-likelihoods). Although this assumption of independence is violated (since these data came from the same replicates), simulations suggest that this violation has a minimal impact on parameter estimates (Abadi *et al.* 2010).

The key additional component of this simultaneous fit is a likelihood function for the parasite consumption data. Integrating each foraging-based transmission model also yields a prediction for the density of parasites remaining after the one day exposure, $Z(1)_{Pred}$. The three foraging-based models provided different predictions for the density of parasites remaining after the one day exposure, $Z(1)_{Pred}$:

Constant foraging: $$Z(1)_{pred} = Z(0)\exp\left(-fS(0)\right) \quad \text{(Eq. S2.4a)}$$

Linear interference: $$Z(1)_{pred} = Z(0)\exp\left(-f(1-c_f S(0))S(0)\right) \quad \text{(Eq. S2.4b)}$$

Exponential interference: $$Z(1)_{pred} = Z(0)\exp\left(-f(\exp(-c_f S(0))S(0)\right) \quad \text{(Eq. S2.4c)}$$

We assumed that the observed density estimates, $Z(1)_{obs}$, were log-normally distributed. Therefore, we assumed that $ln(Z(1)_{obs})$ is normally distributed, with mean = $ln(Z(1)_{pred})$ and a common standard deviation among treatments, s. This provides a likelihood function for the model parameters (along with the common standard deviation, s), given the data and model:

$$\ell_{PC}\left(\text{parameters} \mid \text{data}, \text{model}\right) = \frac{1}{s\sqrt{2\pi}}\exp\left(\frac{\left(\ln\left(Z(1)_{obs}\right) - \ln\left(Z(1)_{pred}\right)\right)^2}{2s^2}\right) \quad \text{(Eq. S2.5)}$$

To find the negative log-likelihood for the parasite consumption (PC) component, $\mathcal{L}_{PC}$, we summed the negative log-likelihood (i.e., $-\ln(\ell_{PC})$) calculated for each replicate tube for using the parasite consumption data (using Eq. S2.5). Following our assumption of independence, the joint negative log-likelihood for a vector of parameters, $\mathcal{L}_J$, is the sum of the negative log-likelihoods for each dataset:

$$\mathcal{L}_J = \mathcal{L}_{INF} + \mathcal{L}_{PC} \quad \text{(Eq. S2.6)}$$

For each foraging-based model we determined the parameter values that minimized this total using the mle2 function of the bbmle package in R (R Development Core Team 2008; Bolker

2012). Next, we obtained 95% confidence intervals for all model parameters via likelihood profiling (Bolker 2008; R Development Core Team 2008) We then ranked the performance of these models with statistics based on AIC (as described in "Competition 1" above).

Additional results – maximum likelihood parameter estimates and model fits

Here we provide supplemental results from the model competition. We provide best-fitting parameters for all models from *Competition 1* in Table S2.1. Further, the best fits obtained for the *Phenomenological* and *Exponential interference* models for *Model Competition* 1 are shown in Figure S2.1. In Table S2.2, we also provide best-fit parameter estimates and 95% confidence intervals for the three foraging-explicit models analyzed in *Model Competition 2*. Additionally, we show the best fit obtained for the *Exponential interference* model in *Model Competition 2* in Figure S2.2.

Table S2.1. Maximum likelihood parameter estimates for all models in *Competition 1* (using only the infection data).

	Parameters (units)		
Model	β **(L spore^{-1} d^{-1})**	p **(unitless)**	q **(unitless)**
Density dependent	7.61×10^{-3}	-	-
Phenomenological	1.88×10^{-3}	-0.28	-0.37
	u **(host spore^{-1})**	f **(L host^{-1} d^{-1})**	c_f **(L host^{-1})**
Constant foraging	1.27×10^{-3}	1.37×10^{-2}	-
Linear interference	2.92×10^{-2}	5.15×10^{-4}	2.62×10^{-3}
Exponential interference	2.71×10^{-2}	6.77×10^{-4}	5.44×10^{-3}

Table S2.2. Maximum likelihood parameter estimates and 95% confidence intervals (in parentheses) for the foraging-explicit transmission models competed in *Competition 2* (using both infection and parasite consumption data).

	Parameters (units)		
Model	u **(host spore^{-1})**	f **(L host^{-1} d^{-1})**	c_f **(L host^{-1})**
Constant foraging	8.44×10^{-4}	9.20×10^{-3}	-
	(6.13×10^{-4} –	(8.06×10^{-3} –	
	1.14×10^{-3})	1.03×10^{-2})	
Linear interference	1.27×10^{-3}	2.67×10^{-2}	3.55×10^{-3}
	(9.87×10^{-4} –	(2.09×10^{-2} –	(2.50×10^{-3} –
	1.27×10^{-3})	3.26×10^{-2})	4.48×10^{-3})
Exponential interference	1.17×10^{-3}	2.17×10^{-2}	1.91×10^{-3}
	(1.03×10^{-3} –	(1.82×10^{-2}–	(1.52×10^{-3} –
	1.31×10^{-3})	2.49×10^{-2})	2.19×10^{-3})

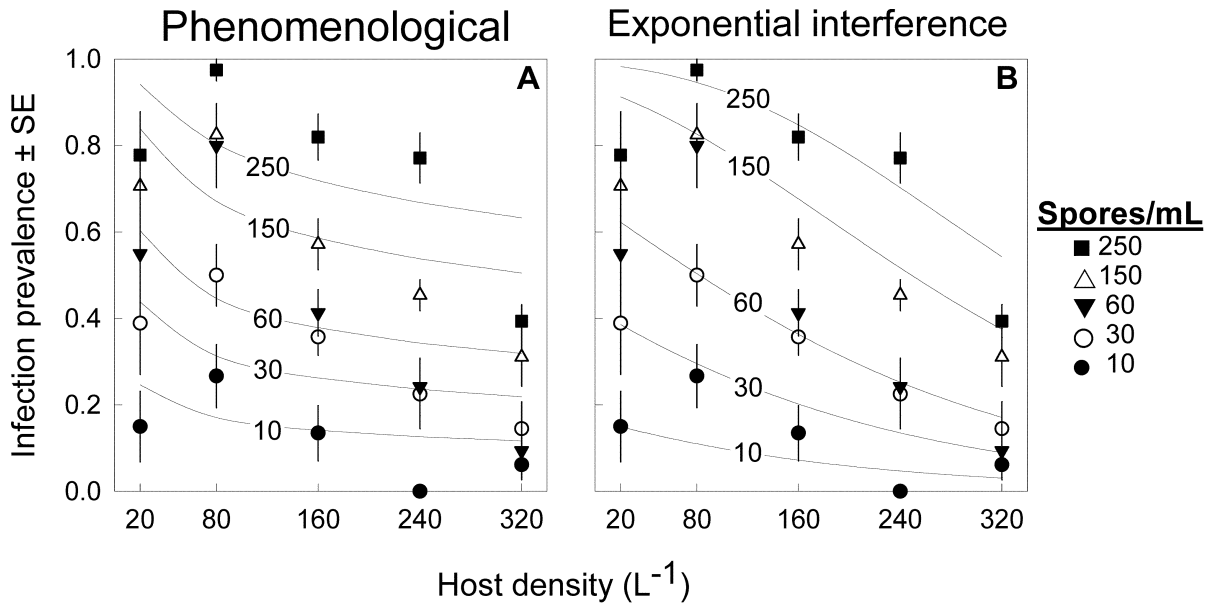

Figure S2.1 Supplementary results for *Competition 1* (infection data only). Best-fit predictions for two additional transmission models for the infection prevalence results (mean ± SE). (A) The *phenomenological* model predicts an initial decrease in infection prevalence with host density, but it overestimates prevalence at the highest density. Overall, this model performs very poorly (See Table 1). (B) The *exponential interference* model fits the data much better. It predicts a more gradual decline in prevalence with host density. This model ranked second, behind only the *linear interference* model.

Figure S2.2

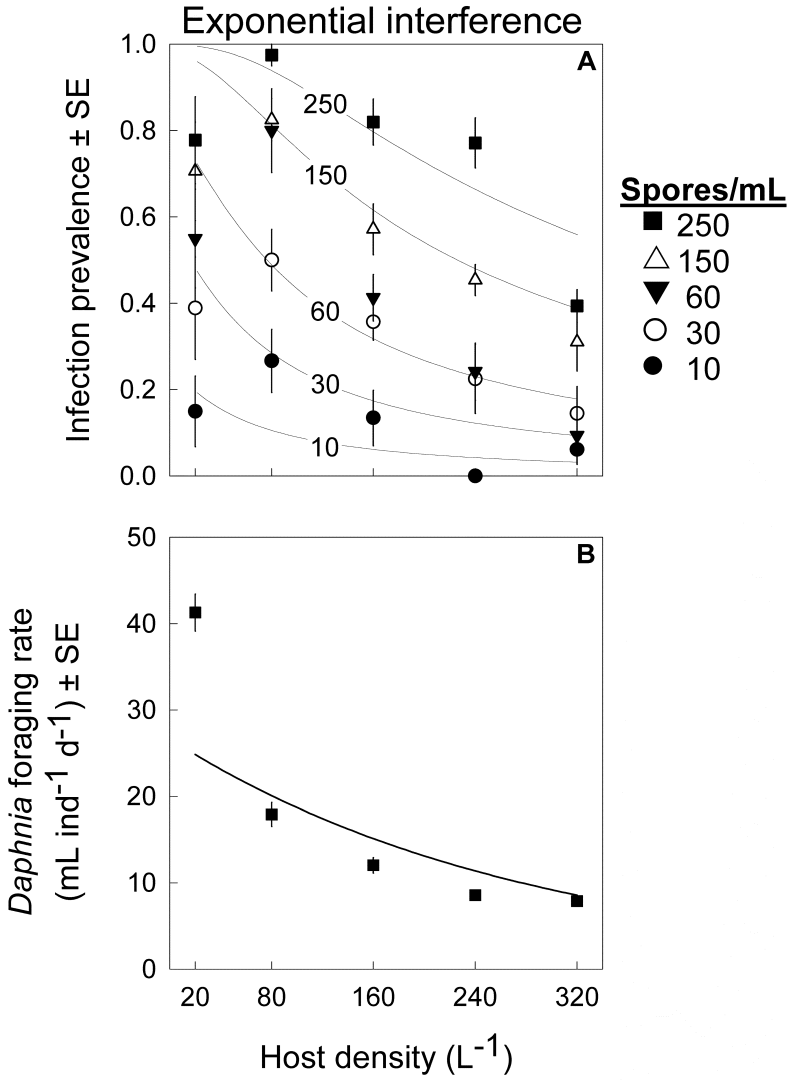

Figure 2.2 Supplementary results for *Competition 2*, using infection and parasite consumption data. (A) The *exponential interference* model fit the infection data well. In general, it captured the decline in infection prevalence (mean ± SE) with increasing host density. (B) Simultaneously, this model captured the decline in the per capita foraging rate of hosts (mean ± SE).

References

1. Abadi F., Gimenez O., Arlettaz R. & Schaub M. (2010). An assessment of integrated population models: bias, accuracy, and violation of the assumption of independence. *Ecology,* 91, 7-14.
2. Ben-Ami F., Regoes R.R. & Ebert D. (2008). A quantitative test of the relationship between parasite dose and infection probability across different host-parasite combinations. *Proc. R. Soc. B,* 275, 853-859.
3. Besbeas P., Freeman S.N. & Morgan B.J.T. (2005). The potential of integrated population modelling. *Aust. & N. Z. J. Stats.,* 47, 35-48.
4. Bolker B. (2012). bbmle: Tools for general maximum likelihood estimation. http://cran.r-project.org/web/packages/bbmle/index.html
5. Bolker B.M. (2008). *Ecological models and data in R*. Princeton Univ Press.
6. Burnham K.P. & Anderson D.R. (2002). Model selection and multimodel inference: a practical information-theoretic approach. Springer-Verlag. *New York*
7. Hall S.R., Sivars-Becker L., Becker C., Duffy M.A., Tessier A.J. & Caceres C.E. (2007). Eating yourself sick: transmission of disease as a function of foraging ecology. *Ecol. Lett.,* 10, 207-218.
8. R Development Core Team (2008). R: A language and environment for statistical computing. R foundation for Statistical Computing. Vienna, Austria.
9. Rachowicz L.J. & Briggs C.J. (2007). Quantifying the disease transmission function: effects of density on *Batrachochytrium dendrobatidis* transmission in the mountain yellow-legged frog *Rana muscosa. J. Anim. Ecol.,* 76, 711-721.

10. Schaub M., Gimenez O., Sierro A. & Arlettaz R.E.L. (2007). Use of integrated modeling to enhance estimates of population dynamics obtained from limited data. *Cons. Biol.,* 21, 945-955.
11. Soetaert K., Petzoldt T. & Setzer R. (2010). Solving differential equations in R: Package deSolve. *J. Stat. Soft.,* 33, 1-25.

Appendix S3: Analytical results for the fully dynamic model – Parasite invasion

In this appendix, we formally derive the R_0 criteria for each of the three fully dynamic epidemiological models considered in the text (Figure 3). The three models follow the same basic structure (Eq. 7) but vary in how transmission rate (T_R) and foraging rate (F_R) are represented (see Table 1). We calculate R_0 for each model using the same method based on eigenvalues of the Jacobian matrix (i.e., stability analysis of the boundary, disease-free equilibrium). We can also derive the same R_0 expressions using the next-generation matrix-based approach (Diekmann et al. 2010). Using the technique from stability analysis, we first calculate the Jacobian matrix for the *S*-*I*-*Z* system, evaluated at the disease-free "boundary" equilibrium ($S = S^*_b$, $I = 0$, $Z = 0$). Regardless of the details of transmission and foraging, S^*_b, remains the same for each model. It is determined by vital rates of the host, b and d, and the strength of density dependence on the host's birth rate, c_b:

$$S^*_b = (b\text{-}d)/(bc_b) \qquad \text{(Eq. S3.1)}$$

Next, we ask if that Jacobian matrix, when considered at the boundary equilibrium, is stable. If it is not (i.e., it has a positive eigenvalue [$\lambda_j > 0$]), then the parasite can invade. We can then rearrange these eigenvalues to determine the parasite's basic reproductive ratio and the threshold host population density required for parasite invasion.

The first model (*density dependent*) considers constant transmission rate ($T_R = \beta$) and no consumption and removal of the parasite ($F_R = 0$). It has a Jacobian matrix, $\mathbf{J_1}$:

$$\mathbf{J_1} = \begin{bmatrix} -(b-d) & b(\rho - c_b(1+\rho)S^*_b) & -\beta S^*_b \\ 0 & -(d+v) & \beta S^*_b \\ 0 & \sigma(d+v) & -m \end{bmatrix}. \qquad \text{(Eq. S3.2)}$$

All three Jacobian matrices have the same basic structure as $\mathbf{J_1}$ shown here, with zeros in the left column (at elements J_{21} and J_{31}). Matrix theory tells us then one of the eigenvalues sits in the upper left corner (element J_{11}) – and this one is always negative (i.e., $\lambda_1 = -(b - d) < 0$), for all three models. The other two eigenvalues come from the four element submatrix in the lower right portion of the Jacobian matrix. Since that submatrix has a trace $\theta_1 = -d - v - m$, we can write the two remaining eigenvalues ($\lambda_{2,3}$) as:

$$\lambda_{2,3} = (1/2)\left(\theta_1 \pm \sqrt{(-\theta_1)^2 + 4(\sigma\beta S_b^* - m)(d + v)}\right) \qquad \text{(Eq. S3.3)}$$

With some algebra, we can see that one of these two eigenvalues is positive when the disease-free host density exceeds a value determined by three epidemiological traits:

$$S_b^* > \frac{m}{\sigma\beta} \qquad \text{(Eq. S3.4)}$$

Rearrangement of this instability (invasion) condition leads to the R_0 expression for the model with classic density dependent transmission:

$$R_{0,1} = \left(\frac{\sigma\beta}{m}\right) S_b^* \qquad \text{(Eq. S3.5)}$$

This equation shows how R_0 increase with host density (Figure 3A-B) with slope $\sigma\beta/m$.

In the second model (*constant foraging*), we assume parasite (spore) removal with exposure. Thus, the Jacobian matrix changes to $\mathbf{J_2}$:

$$\mathbf{J_2} = \begin{bmatrix} -(b - d) & b(\rho - c_b(1 + \rho)S_b^*) & -ufS_b^* \\ 0 & -(d + v) & ufS_b^* \\ 0 & \sigma(d + v) & -(fS_b^* + m) \end{bmatrix}. \qquad \text{(Eq. S3.6)}$$

Notice how the transmission rate parameter, β, has been replaced with the more mechanistic product uf. Additionally, there is an additional loss term in the bottom-left corner (element J_{33}) due to consumption of spores by hosts. Like in the first model, the two remaining eigenvalues come from the four elements in the lower right part of this matrix $\mathbf{J_2}$. If that associated trace of $\mathbf{J_2}$ is $\theta_2 = -d - v - m - f S_b^*$, then the two eigenvalues are:

$$\lambda_{2,3} = (1/2)\left(\theta_2 \pm \sqrt{(-\theta_2)^2 + 4\left(fS_b^*(\sigma u - 1) - m\right)(d + v)}\right) \quad \text{(Eq. S3.7)}$$

One of the eigenvalues is positive (i.e., the parasite can invade), when host density surpasses a minimum threshold:

$$S_b^* > \frac{m}{f(\sigma u - 1)} = \frac{m}{(\sigma\beta - f)} \quad \text{(Eq. S3.8)}$$

Once we remember $\beta = uf$, we see that the threshold density for this model is always higher than the threshold for the density dependent transmission model (since the denominator in Eq. S3.8 is smaller than that in Eq. S3.4). Thus, the added source of mortality for parasite spores (i.e., consumption of spores by both host classes) tends to inhibit parasite invasion. Rearrangement of this invasion criterion leads to the R_0 equation for the *constant foraging* model:

$$R_{0,2} = \frac{f}{m}(\sigma u - 1)S_b^* = \left(\frac{\sigma\beta - f}{m}\right)S_b^* \quad \text{(Eq. S3.9)}$$

The R_0 quantity still increases (linearly) with host density, but with a smaller slope (Eq. S3.9 term in parentheses) compared with the density dependent model (Eq. S3.5).

The third model (*linear interference*) combines foraging by hosts with a decline in the foraging (exposure) rate with host density. The Jacobian matrix for this model ($\mathbf{J_3}$) becomes:

$$\mathbf{J_3} = \begin{bmatrix} -(b-d) & b\left(\rho - c_b(1+\rho)S_b^*\right) & -uf\left(1 - c_f S_b^*\right)S_b^* \\ 0 & -(d+v) & uf\left(1 - c_f S_b^*\right)S_b^* \\ 0 & \sigma(d+v) & -f\left(1 - c_f S_b^*\right)S_b^* - m \end{bmatrix}. \qquad \text{(Eq. S3.10)}$$

Note an important change in the structure of this Jacobian matrix: element J_{23} introduces the square of host density, $(S_b^*)^2$. This squared term will produce the unimodal R_0 expression that arises below. Following the same procedure as before, after we define the trace of the pertinent submatrix as $\theta_3 = -d - v - m - f(1 - c_f S_b^*)\, S_b^*$, the relevant eigenvalues become:

$$\lambda_{2,3} = (1/2)\left(\theta_3 \pm \sqrt{(-\theta_3)^2 + 4\left(fS_b^*\left(1 - c_f S_b^*\right)(\sigma u - 1) - m\right)(d+v)}\right) \qquad \text{(Eq. S3.11)}$$

Some algebra reveals that one of the eigenvalues is positive when host density sits in between two solutions:

$$S_b^* = \frac{1}{2c_f}\left(1 - \sqrt{\left(1 - \frac{4c_f m}{f(\sigma u - 1)}\right)}\right) \qquad \text{(Eq. S3.12.a)}$$

$$S_b^* = \frac{1}{2c_f}\left(1 + \sqrt{\left(1 - \frac{4c_f m}{f(\sigma u - 1)}\right)}\right) \qquad \text{(Eq. S3.12.b)}$$

Under the *linear interference* transmission model, two density thresholds now arise. The smaller threshold (Eq. S3.12.a) is qualitatively analogous to that observed in the two simpler models (i.e., it must be exceeded for parasite invasion). Some more algebra (not shown) indicates that this smaller threshold exceeds the single threshold under the *constant foraging* model (S3.8) – as it should, since now two components of host biology (spore consumption plus foraging interference) impeded transmission. However, the larger threshold (Eq. S3.12.b) means that the population can become too dense for the parasite to invade. This upper threshold arises because

strong interference at high host density can depress host – parasite contact rates enough to impede invasion of the parasite.

These threshold population sizes (equ. S3.12) produce an expression for R_0 that is quadratic with respect to host density (S_b^*):

$$R_{0,3} = \frac{f(\sigma u - 1)}{m}\left(S_b^* - c_f S_b^{*2}\right) = R_{0,2}\left(1 - c_f S_b^*\right) \qquad \text{(Eq. S3.13)}$$

The linear term is the R_0 expression for the *constant foraging* model ($R_{0,2}$; defined in Eq. S3.9). But, now that inference has been introduced, the new R_0 is ultimately unimodal: for biologically feasible parameters, R_0 is concave down (i.e., $d^2R_0/dS^*_b{}^2 < 0$). Thus, R_0 in the *linear interference* model is maximized at intermediate host density.

This R_0 expression for the linear interference model prompts an additional, theoretically relevant point. The R_0 curve responds unimodally (Eq. S3.13) because of the introduction of inference biology (in element J_{23} in Eq. S3.10), not due to the parasite consumption biology. For the sake of thoroughness, we can demonstrate this conclusion by analyzing a model with only interference in foraging rate but no spore consumption. (Our data clearly contradict this assumption [Figure 2], but this case may apply to other systems, so it is worth considering beyond the math). The Jacobian becomes:

$$\mathbf{J_4} = \begin{bmatrix} -(b-d) & b\left(\rho - c_b(1+\rho)S_b^*\right) & -uf\left(1 - c_f S_b^*\right)S_b^* \\ 0 & -(d+v) & uf\left(1 - c_f S_b^*\right)S_b^* \\ 0 & \sigma(d+v) & -m \end{bmatrix}. \qquad \text{(Eq. S3.14)}$$

Note the host-squared term again in element J_{23}. This variant on the model also yields a unimodal R_0 expression (after calculating the eigenvalues, as above):

$$R_{0,4} = \frac{\sigma u f}{m}\left(S_b^* - c_f S_b^{*2}\right) = R_{0,1}\left(1 - c_f S_b^*\right) \qquad \text{(Equ. S3.15)}$$

Thus, if host interference reduces exposure to parasites, a unimodal R_0 expression may arise – even if hosts do not effectively deplete free-living stages of the parasite.

REFERENCES

1. Diekmann, O., Heesterbeek, J.A.P., & Roberts, M.G. (2010). The construction of next-generation matrices for compartmental epidemic models. *J. R. Soc. Interface*. 7, 873-885.